Journal of Pharmaceutical and Biomedical Analysis 180 (2020) 113050

Contents lists available at ScienceDirect

Journal of Pharmaceutical and Biomedical Analysis

journal homepage: www.elsevier.com/locate/jpba

pDNA conjugated with citrate capped silver nanoparticles towards ultrasensitive bio-assay of *haemophilus influenza* in human biofluids: A novel optical biosensor

Soodabeh Hassanpour[a], Arezoo Saadati[b,c], Mohammad Hasanzadeh[d,*]

[a] Department of Analytical Chemistry, Faculty of Science, Palacky University Olomouc, 17. Listopadu 12, 77146 Olomouc, Czech Republic
[b] Biotechnology Research Center, Tabriz University of Medical Sciences, Tabriz, Iran
[c] Nutrition Research Center, Tabriz University of Medical Sciences, Tabriz, Iran
[d] Pharmaceutical Analysis Research Center, Tabriz University of Medical Sciences, Tabriz, Iran

ARTICLE INFO

Article history:
Received 3 November 2019
Received in revised form 9 December 2019
Accepted 17 December 2019
Available online 19 December 2019

Keywords:
DNA bio-assay
Citrate capped silver nanoparticle
Haemophilus influenza
Fluorescence
Human biofluids
Genosensor

ABSTRACT

A sensitive and specific approach was developed for the determination of *Haemophilus influenza* using DNA based bio-assay. In this study, citrate capped silver nanoparticle was synthesized and employed for bioconjugation with pDNA toward target sequences detection. In this study, synthesized probe (SH-5′-AAT TTT CCA ACT TTT TCA CCT GCA T-3') of *Haemophilus influenza* was detected with great sensitivity and selectivity after hybridization with cDNA (5′-ATG CAG GTG AAA AAG TTG GAA AAT T-3'). Regarding to the obtained results, the low limit of quantification (LLOQ) of DNA sample was 1 ZM using 15 μL of probe and 200 μL of Cit/AgNPs. According to ultra-sensitivity of the fabricated optical DNA-based bio-assay, it has potential for bacterial determination both in clinical and environmental specimens. To evaluate the selectivity of developed DNA based biosensor, three mismatch sequences were applied. Finally, the designed genosensor is a significant diagnostic strategy for detection of *Haemophilus influenza* with great selectivity.

1. Introduction

Haemophilus influenza (*H. influenza*) is a gram negative coccobacillus which produces polysaccharide capsules. There are 6 serotypes from A to F based on type of capsular antigen [1]. Capsulated strains are resistant towards phagocytosis, whereas non-capsulated strains have less resistance and invasive features [2]. *Influenza* causes respiratory infections including; bronchitis, acute otitis media, pneumonia, and sinusitis. Furthermore, it leads to invasive infections like meningitis, septic arthritis, and cellulite [3]. Hence, sensitive and fast determination of *H. influenza* is of paramount significance in medical microbiology. There are numerous techniques for diagnosis of *H. influenza* such as Polymerase chain reaction (PCR), latex particle agglutination (LAT), and culture. The latex particle agglutination and culture techniques are usually employed for clinical diagnosis of viruses [4,5]. *H. influenza* is still a fastidious bacterium and its growing needs compound nutrition. Replication of this virus takes long time, so in culture technique it may takes long period of time up to weeks. A more sensitive method than culture and LAT is PCR but it also has some limitations. Some disadvantages of these methods are being laborious, time-consuming, low specificity and sensitivity as well as requiring developed high-price instruments and expert technicians [6].

Because of limitations of conventional techniques in detection of biological molecules (specially *H. influenza*), biosensors have been utilized for specific and more sensitive detection of *H. influenza* [7]. Genosensors are usually applied for detection of infectious diseases [8,9]. Recently, DNA-based biosensors or genosensors have been widely utilized for detection because of their great sensitivity, specificity, low-cost, simplicity as well as minimization ability [10]. Hybridization of DNA is the most significant process in the fabrication of DNA-based biosensors in which ssDNA (single-stranded DNA) immobilizes on the on the surface nanoparticle and target DNA (cDNA) bind to it for forming double-stranded helix (ds-DNA) [11,12]. By emerging of nanotechnology, various kinds of nanoparticles are applied for immobilization of thiolated DNA probe with exceptional attributes like great adsorption power, great surface area and biocompatibility. Among the metallic nanoparticles, AgNPs (silver nanoparticles) have been broadly

* Corresponding author.
E-mail addresses: hasanzadehm@tbzmed.ac.ir, mhmmd_hasanzadeh@yahoo.com (M. Hasanzadeh).

https://doi.org/10.1016/j.jpba.2019.113050
0731-7085/

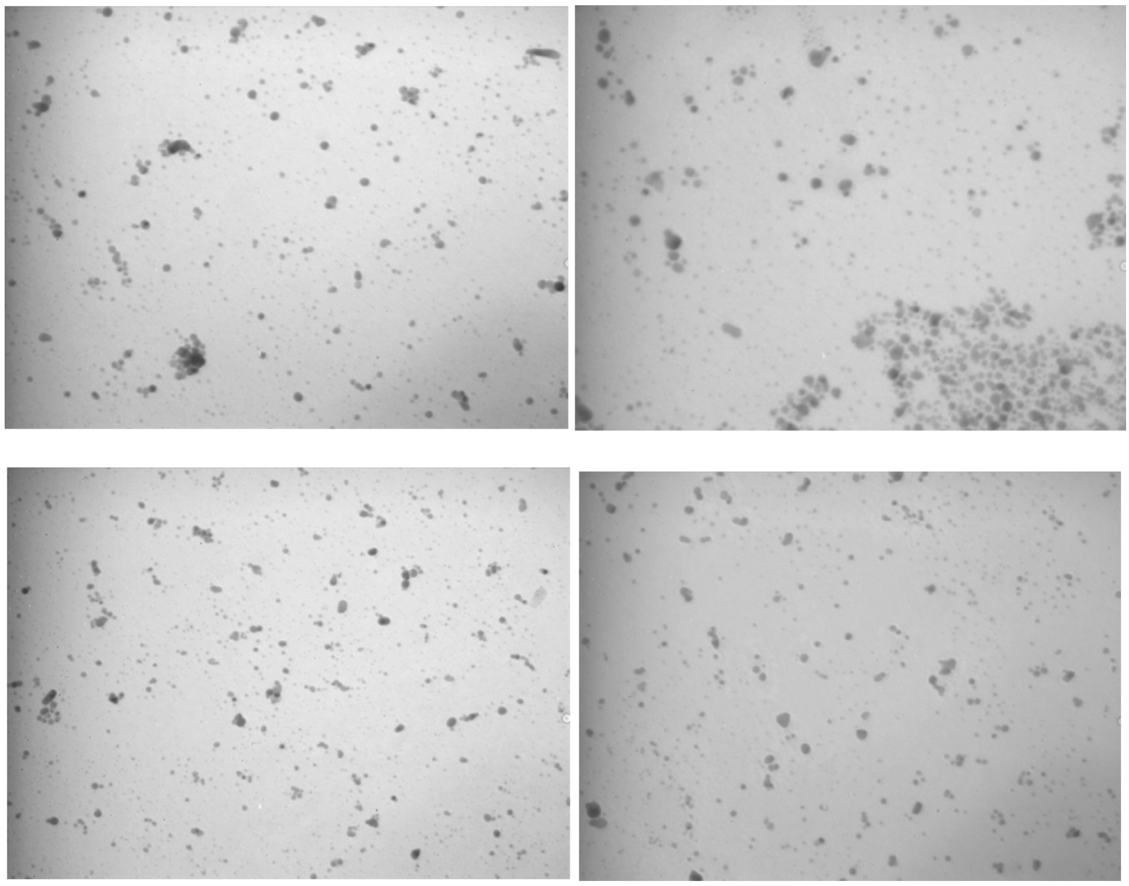

Fig. 1. TEM images of Cit/AgNPs in various magnifications.

examined mostly because of their unique and optical characteristics as well as excellent extinction coefficients [13–15]. AgNPs draw lots of interests for its application in optical sensors because of their simple and cheap fabrication besides their greater extinction coefficients than those of gold nanoparticles with the similar average size [14,15]. In addition, the high surface area of AgNPs is completely appropriate for modification and fabricate useful components in colorimetric determination of some analytes.

It is important to point out that, the aggregation of organic dyes with aggregation-induced emission (AIE) have also be used widely for biological imaging and sensing applications [16–25]. In future, their applications especially in biomedical analysis could be cited.

In present research, an innovative optical DNA-based biosensor using citrate capped silver nanoparticles for detection of *H. influenza* gene was developed. The purpose of this study is design a spectrofluorometeric and UV/Vis spectrophotometric technique for sensitive determination of *H. influenza*. The developed method not only has acceptable linear range but also it is simple and cost-efficient technique in comparison with conventional methods.

2. Method and materials

2.1. Chemical and reagents

Sodium acetate (CH_3COONa), sodium chloride (NaCl), DTT (Dithiotrietol), silver nitrate ($AgNO_3$), $NaBH_4$ (sodium borohydride), trisodium citrate ($Na_3C_6H_5O_7$) were purchased from Sigma-Aldrich (Ontario, Canada). The oligonucleotide sequences achieved from Takapouzist Co. (Iran) include:

- Probe single strand DNA (ssDNA): SH-5′-AAT TTT CCA ACT TTT TCA CCT GCA T-3’
- Complementary target DNA: 5′-ATG CAG GTG AAA AAG TTG GAA AAT T-3’
- 1-base mismatched target DNA: 5′-ATG GAG GTG AAA AAG TTG GAA AAT T-3’
- 2-base mismatched target DNA: 5′-AGG GAG GTG AAA AAG TTG GAA AAT T-3’
- 3-base mismatched target DNA: 5′-AGG GAG GTG AGA AAG TTG GAA AAT T-3’

Dilution of oligonucleotides was performed using Tris–HCl buffer (0.1 M, pH∼7.4). DTT solution was made ready using 500 mM DTT and 10 mM sodium acetate (pH∼5.2).

2.2. Apparatus

Transmission electron microscopy (TEM) was carried out by Philips CM30 electron microscope operated at 200 kV (Adelaide, Australia). Dynamic light scattering (DLS) was evaluated using zeta potential instrument Malvern Instruments Ltd (Zetasizer Ver. 7.11, MAL1032660, England) for size distribution and zeta potential. Field emission scanning electron microscope (FE-SEM) (Hitachi-SU8020, Czech) with an operating voltage of 3 kV was performed to appraise the modified electrode surface and particles morphology. The chemical composition of the modified electrodes was investigated using energy dispersive spectroscopy (EDS). Overall these instruments have three major components-laser, sample and light detector UV-VIS spectrophotometer achieved by shimadzu UV-1800 UV-VI spectrophotometer with a resolution of 1 nm. Fluorescence spectra and intensity measurements were done

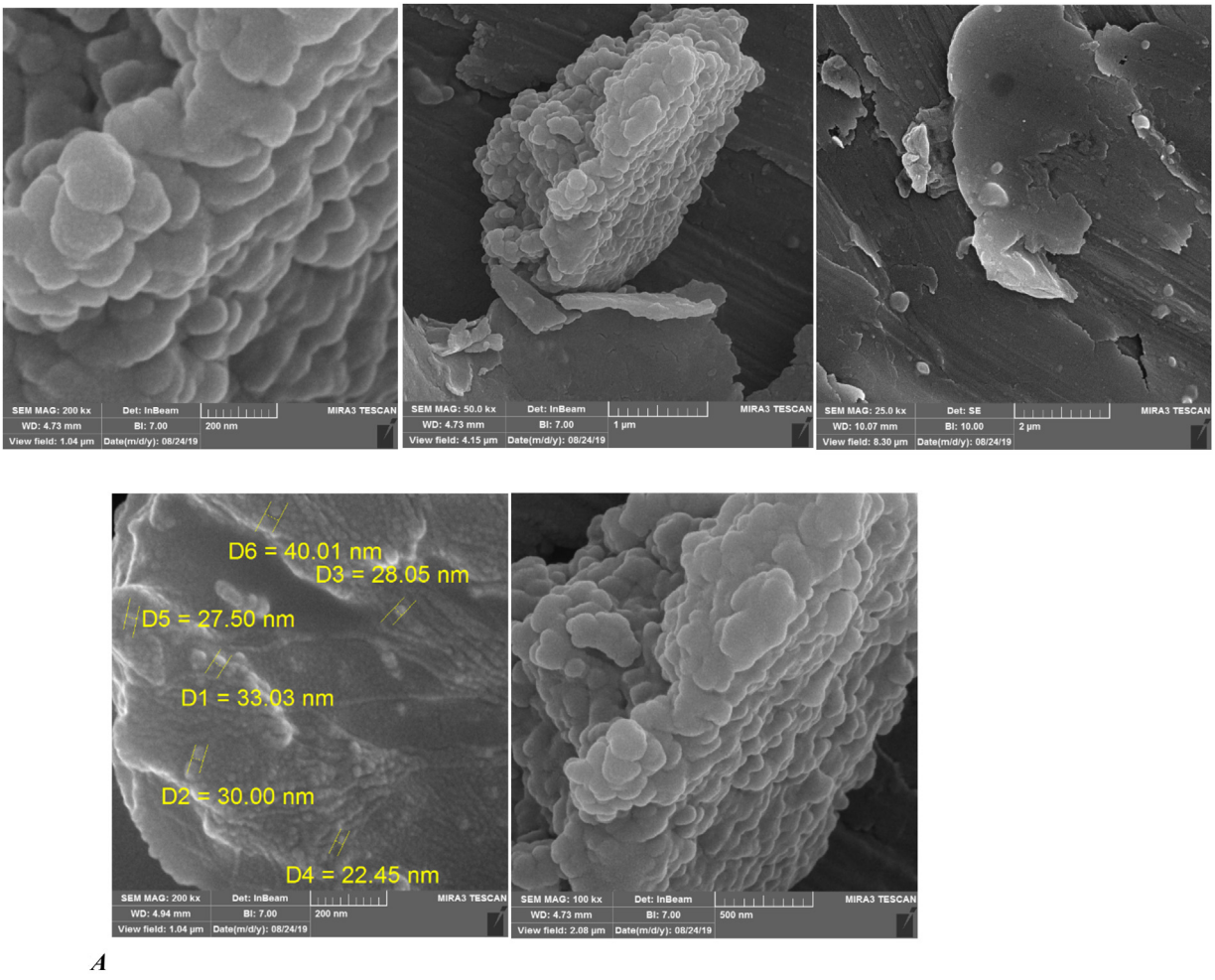

Fig. 2. (A). FE-SEM images of Cit/AgNPs in various magnification. (B). EDS spectra of Cit/AgNPs.

employing a Jasco FP-750 Spectrofluorometer (Japan) equipped 1.0 cm quartz cells and a 150 W xenon lamp.

2.3. Synthesis of citrate capped silver nanoparticles

In order to synthesis the citrate capped silver nanoparticles, in an ice bath (approximately 0 °C) 400 mL of trisodium citrate (1.06 mM) solution, as a capping/stabilizing agent, was completely mixed with 25 mL of silver nitrate solution (5 mM). Next, 2500 µL of 100 mM $NaBH_4$ aqueous solution as a reducing agent was drop wisely added to the mixed solution over 5 min. This was led to immediate color alteration to light yellow. The prepared solution was vigorously stirred about 1 h and 45 min under dark condition until the color was shiny yellow which confirms the end of reaction and Cit/AgNPs formation. Then, the ice bath was removed and solution was kept in dark condition overnight to attain room temperature. The synthesized Cit/AgNPs were centrifuged at 6000 rpm for 15 min.

Citrate ions are usually utilized as a reductant and stabilizer in synthesis of metal nanoparticles and makes powerful surface interaction with AgNPs. Adding citrate ions to the silver solution leads to the citrate ions complication with silver nanoparticles. The com-

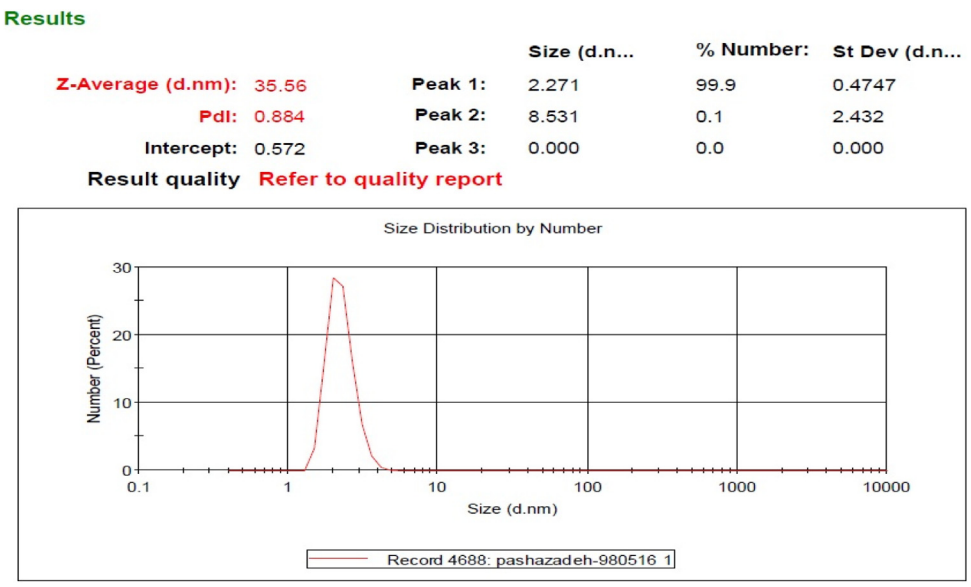

Fig. 3. Size distribution analysis of Cit/AgNPs via DLS.

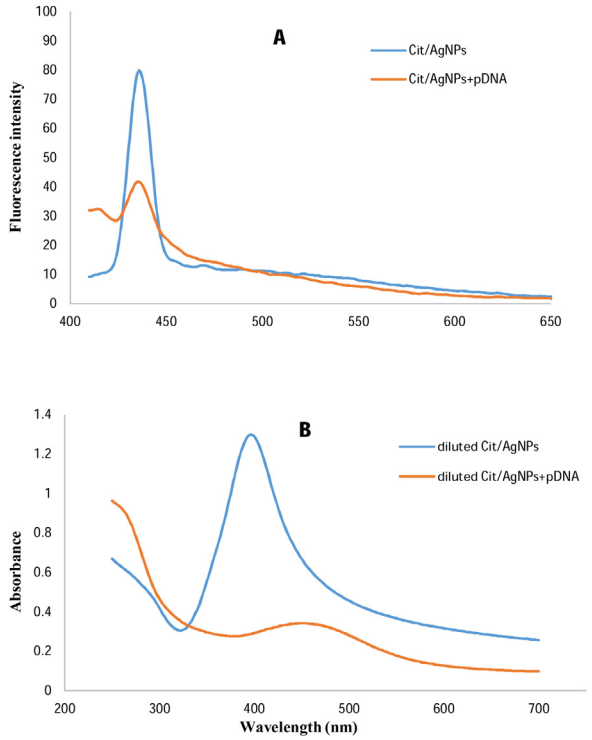

Fig. 4. A) Fluorescence spectra of Cit/AgNPs and Cit/AgNPs-pDNA. B) UV/Vis absorbance spectrum of Cit/AgNPs and Cit/AgNPs-pDNA.

plexity of citrate ions with AgNPs serves significant role in dictating shape and size of AgNPs. Citrate ions effects the growth of particle through compounding with positively charged dimers of Ag^{+} [15].

2.4. TEM, FE-SEM and DLS analysis of citrate capped AgNPs

The mechanism of Cit/AgNPs formation and supportive proof of morphologies and characteristics of silver nanoparticles was provided by TEM (transmission electron microscopy). TEM is continuously the first method employed for determination of the size and nanoparticle size distribution [26]. TEM images recorded using the holey carbon grid which are shown in Fig. 1. The TEM micrographs of synthesized citrate capped silver nanoparticles clearly show the AgNPs are discrete, monodisperse, and spherical in environment with average particle size under 10 nm.

Surface morphology of Cit/AgNPs was characterized by FE-SEM (field emission scanning electron microscope) and chemical compositions of nanoparticles were analyzed by EDS (energy dispersive spectroscopy). As shown in Fig. 2(A), AgNPs have uniform spherical structure. According to the standard theory of colloids, the stability of colloids depends on the equilibrium between the van der Waals interaction and the coulombic repulsion of the charged particles [27]. According to Fig. 2(B), sharp and large peaks from citrate and sodium appear due to the existence of sodium citrate and sodium borohydride in the structure of Cit/AgNPs.

DLS (dynamic light scattering) is a powerful technique which depends on the interaction of light with particles. This technique can be employed for measurements of narrow particle size distributions especially in the range of 2–500 nm [28]. For determination of citrate capped AgNPs hydrodynamic sizes and zeta potential were evaluated (Fig. 3). The average particle size of synthesized Cit/AgNPs was 2.27 nm. Furthermore, Cit-AgNPs exhibits fluorescence emission in the range of 400–600 nm. This may be due to citrate in the structure of this probe with the maximum excitation and emission wavelength at 370 nm and 420 nm, respectively UV–Vis spectra revelled that maximum absorption of Cit-AgNPs is around 397 nm.

3. Results and discussion

3.1. Preparation of optical biosensor

pDNA is one of the most significant element in genosensing. For this purpose, pDNA was activated through combination with DTT. DTT (dithiotrietol) is usually employed as a deprotecting or decreasing agent for thiolated-probe DNA. The sulfur atoms in terminal of thiolated DNA have potential for forming dimers especially in the existence of oxygen. Thiol groups oxidation prevented by DTT. So, it is applied as a protecting agent [29,30]. Therefore, DTT (0.01 M) and sodium acetate (0.01 M) were prepared with deionized water. Then, 15 μL of pDNA (SH-5′-AAT TTT CCA ACT TTT TCA CCT GCA T-3') was mixed with 100 μL DTT/sodium acetate solution. After 15 min, 200 μLof ethyl acetate was added and for 5 min vortexed. The prepared solution was cen-

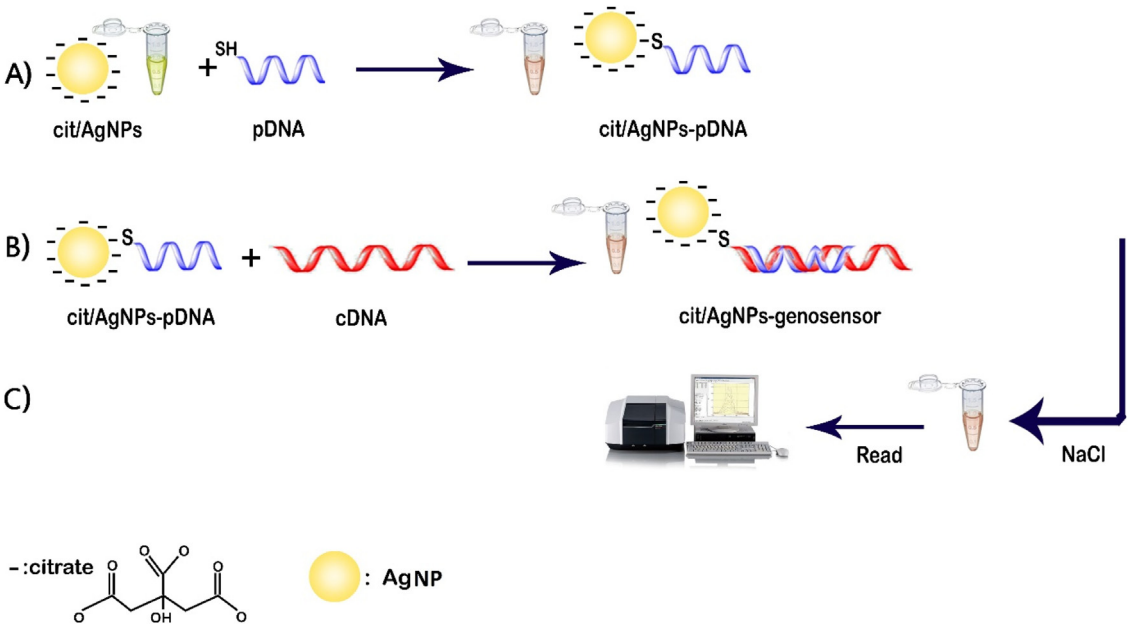

Scheme 1. Illustration of preparation steps of genosensor.

trifuged for 10 min at 8000 rpm and supernatant was removed. Subsequently, 200 μL of Cit/AgNPs was added to the prepared pDNA solution and incubated for 2 h at 45° for spectrofluorometery and 200 μL of diluted Cit/AgNPs (1/2 concentration) was also another microtube of prepared pDNA and incubated which was applied for UV–vis spectrophotometery. 10 μL of NaCl (1 M) was added to 300 μL of mixed Cit/AgNPs-pDNA and Cit/AgNPs for increment of quality and stability of nanoparticles. Then, the prepared solutions were pipetted in the cuvettes and data was recorded both by spectrofluorometer in range of 400–750 nm wavelength and UV-VIS spectrophotometer in range of 250–700 nm spectral range. Fluorescence emission and excitation spectra of Cit/AgNPs and Cit/AgNPs-pDNA are demonstrated in Fig. 4A. The excitation peaks for Cit/AgNPs and Cit/AgNPs-pDNA were observed at 439 and 438 nm, respectively. The fluorescence spectrum of Cit/AgNPs was similar to that of Cit/AgNPs-pDNA; although, the fluorescence intensity was declined by pDNA. As can be seen in Fig. 4B, momentous alteration in UV–vis spectra was happened after addition of pDNA which appeared at 470 nm. All of the genosensor preparation steps was shown in Scheme 1.

3.2. Optimization of hybridization time

Hybridization lead to quick and effective binding of DNA strands. In this study, pDNA hybridized with its specific DNA (cDNA (complementary target sequences)). Oligonucleotides were successfully immobilized on the surface of Cit/AgNPs due to interaction of AgNPs surface with oligonucleotides binding groups. Thiol groups of oligonucleotides result in increment of binding affinity of them to the surface of nanoparticles, which leads to greater stability of Ag nanoparticle probes [15]. The Cit/AgNPs have stability toward salt concentration (NaCl). So, they are stable against aggregation by NaCl concentration. This hybridization process was associated with color alteration, red-shifting as a result of assembly of particle which can be seen by naked eye in the form of yellow to pale red color change (Fig. 5A). To evaluate the hybridization and optimum incubation time, Cit/AgNPs functionalized with pDNA (SH-5′-AAT TTT CCA ACT TTT TCA CCT GCA T-3') solution (Cit/AgNPs-pDNA) and incubated with 15 μL of cDNA (5′-ATG CAG GTG AAA AAG TTG GAA AAT T-3') at different incubation times (2, 5, 10, 15, and 20 min). In this part, 10 μL of NaCl was added to enhance the AgNPs stability and inhibted their aggregration. After insertion of 10 μl NaCl, UV–vis spectra was recorded at different time (251,015 and 20 min). Obtained results demonstrated that the optimum cDNA incubation time was 2 min. As revealed in Fig. 5, the location of peak is absolutely similar with previous section.

3.3. Analytical study

Sensitivity is one of the significant parts of the genosensors. In order to evaluate the sensitivity of prepared genosensor, various concentration of cDNA (10^{-6},10^{-9},10^{-12},10^{-15},10^{-17} and 10^{-21} M) was applied with 2 min incubation time. Same as the previous section, 10 μL of NaCl was added for increasing quality and stability of AgNPs. 15 μL of these concentration was added to the prepared Cit/AgNPs-pDNA and incubated at 37° for 2 min. As exhibited in Fig. 6, the maximum peak was recorded for concentration 10^{-6} M and it was thoroughly predictable. According to decrease of cDNA concentration, the intensity of the excited fluorescence and absorbed signal was decreased. According to the results, in spite of recorded signals downward mobility, the developed optical genosensor can be employed for determination of cDNA, target sequence, up to the concentration of 1 ZM for both spectrofluorometer and UV–vis spectrophotometer. Dynamic linear ranges for both were btween 1 μM- 1 zM and regression equations recorded for spectrofluorometery and UV–vis spectrophotometery respectively were:

$$y = -1.7625_{(Haemophilusinfluenza)} + 23.969 R^2 = 0.8412$$

$$y = -0.0885_{(Haemophilusinfluenza)} + 1.1295 R^2 = 0.8692$$

Briefly, the designed DNA based biosensor not only possess great sensitivity but also has easy and low-cost construction.

3.4. Selectivity

One of the remarkable merits of biosensors is its selectivity. Hence, a perfect biosensor should have power to distinguish similar analytes. For evaluate the selectivity, we designed three mismatch sequences (mismatch 1: 5′-ATG GAG GTG AAA AAG TTG GAA AAT

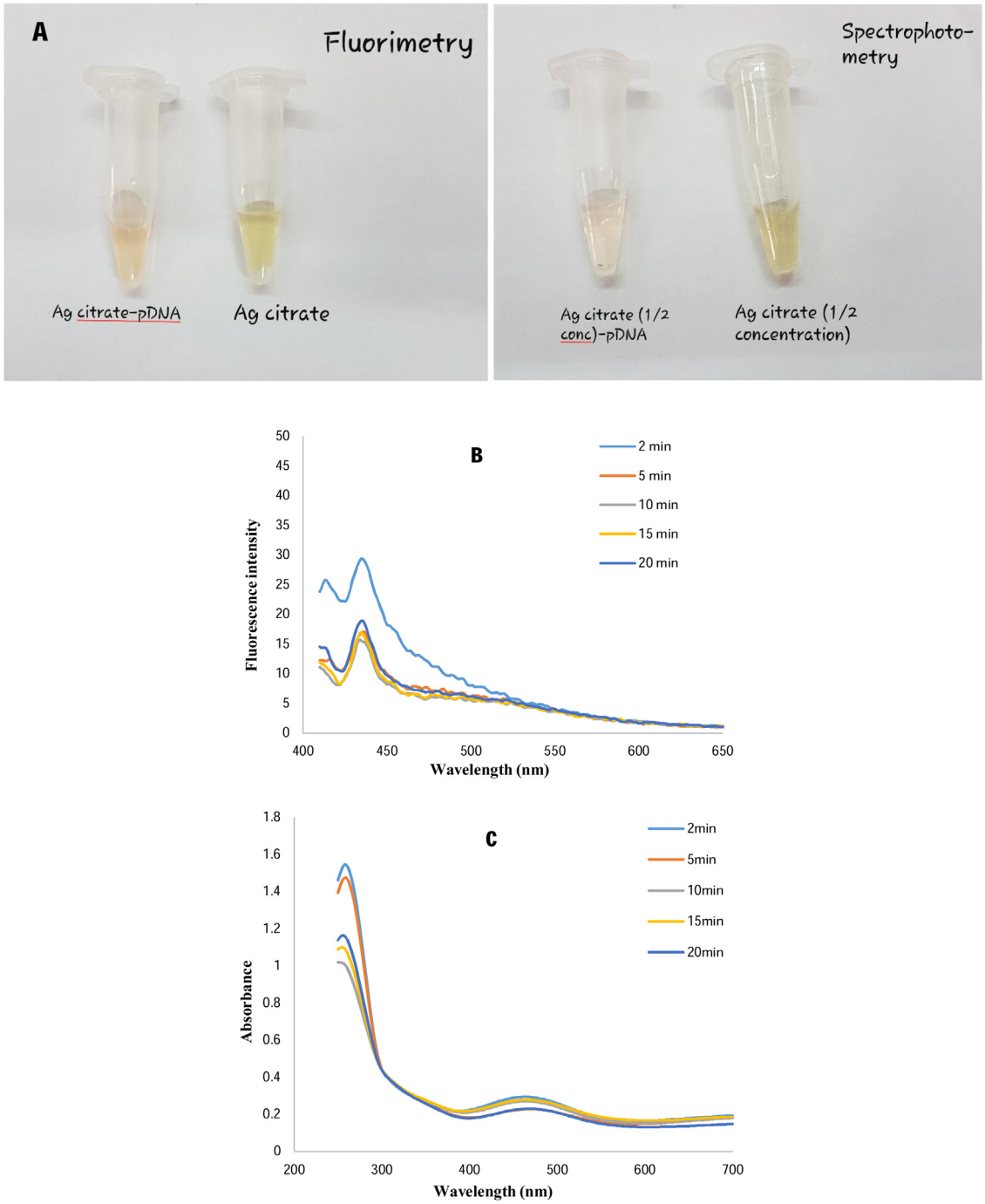

Fig. 5. (A) color alteration of Cit/AgNPs from yellow to pale red after hybridization with pDNA. Fluorescence excitation (B) and UV/Vis absorbance (C) spectrum in various hybridization time (2,5,10,15, and 20 min) (For interpretation of the references to colour in this figure legend, the reader is referred to the web version of this article).

T-3', mismatch 2: 5′-AGG GAG GTG AAA AAG TTG GAA AAT T-3', mismatch 3: 5′-AGG GAG GTG AGA AAG TTG GAA AAT T-3'). Alike with analytical study, the designed genosensor was incubated with 15 μL mismatch primers and fluorescence excitation and UV/Vis absorbance was recorded for comparison with cDNA hybridization. The selectivity of genosensor was evaluated in spectral ranges 400−750 nm and 250−700 nm, respectively. As showed in Fig. 7, in the presence of mismatched DNAs, fluorescence excitation had significant reduction, whereas, UV/Vis absorbance was considerably increased from mismatch one to mismatch three. These results has exact agreement with different reported studies that the dsDNA intensity is more than that of ssDNA.

3.5. Stability

One of the ways to increase the genosensors stability is employing silver nanoparticles. Silver nanoparticles draw a lot of attention in optical biosensors because of their simple and low-cost fabrication as well as great extinction coefficients. In addition, AgNPs has great superficial area which can be suitably modified [14,15]. The stability of developed genosensor was measured in two steps. At first, intraday stability of synthesized Cit/AgNPs was examined at regular 2 -h interval time. According to Fig. 8A-B, the fluorescence excitation and UV/Vis absorbance of Cit/AgNPs were decreased respectively during each 2 -h interval time. In the second step, the

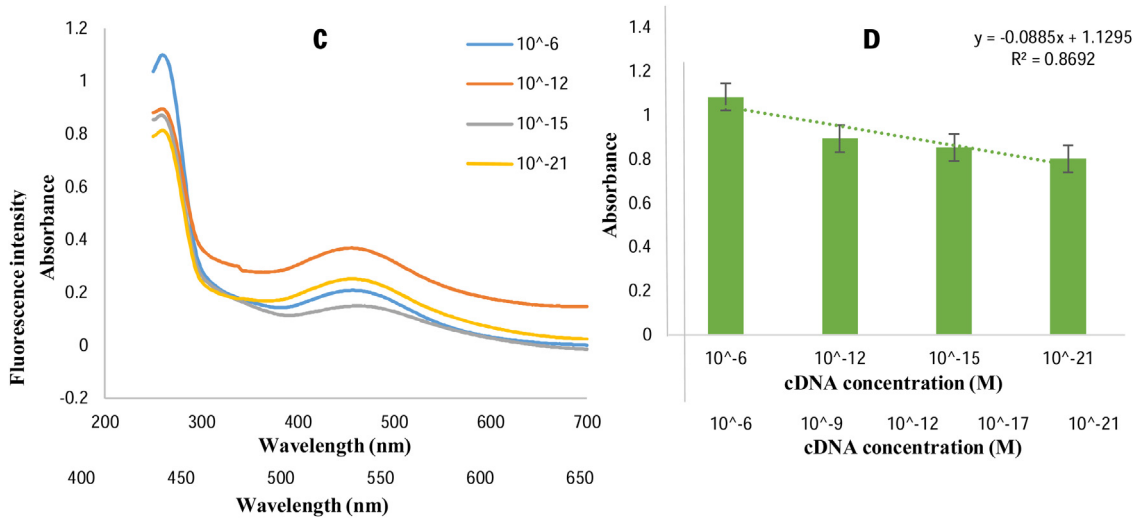

Fig. 6. Fluorescence excitation (A) and UV/Vis absorbance (C) spectrum of genosensor after hybridization with a variety of cDNA concentrations (10^{-6},10^{-9},10^{-12},10^{-15},10^{-17} and 10^{-21} M) in the 400–750 nm and 250–700 nm spectral ranges, respectively. Histograms of peak intensity versus concentration of cDNA (C and D).

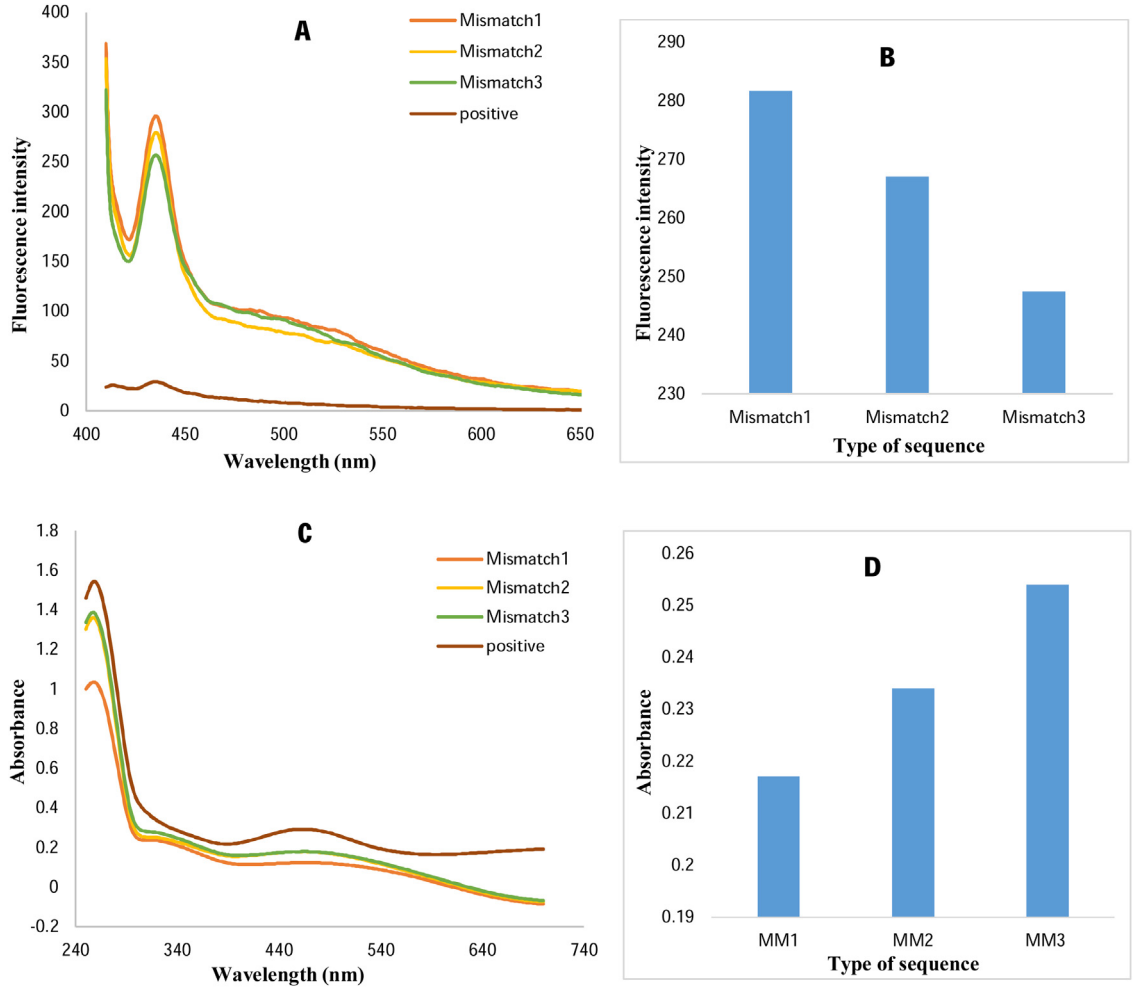

Fig. 7. Fluorescence excitation (A) and UV/Vis absorbance (C) spectrum of hybridization with mismatch cDNAs (Mismatch1, Mismatch2, Mismatch3) in the 400–750 nm and 250–700 nm spectral ranges, respectively. Histograms of peak intensity versus type of sequence (B and D).

stability of developed genosensor was evaluated similar to that of Cit/AgNPs. As displayed in Fig. 8C-D, the fluorescence excitation of engineered genosensor was increased respectively during each 2 -h interval time; whereas, its UV/Vis absorbance was decreased. Therefore, the synthesized Cit/AgNPs has acceptable stability. The genosensor has stability for use within 4 h. Finally, designed platform has appropriate stability despite its easy fabrication.

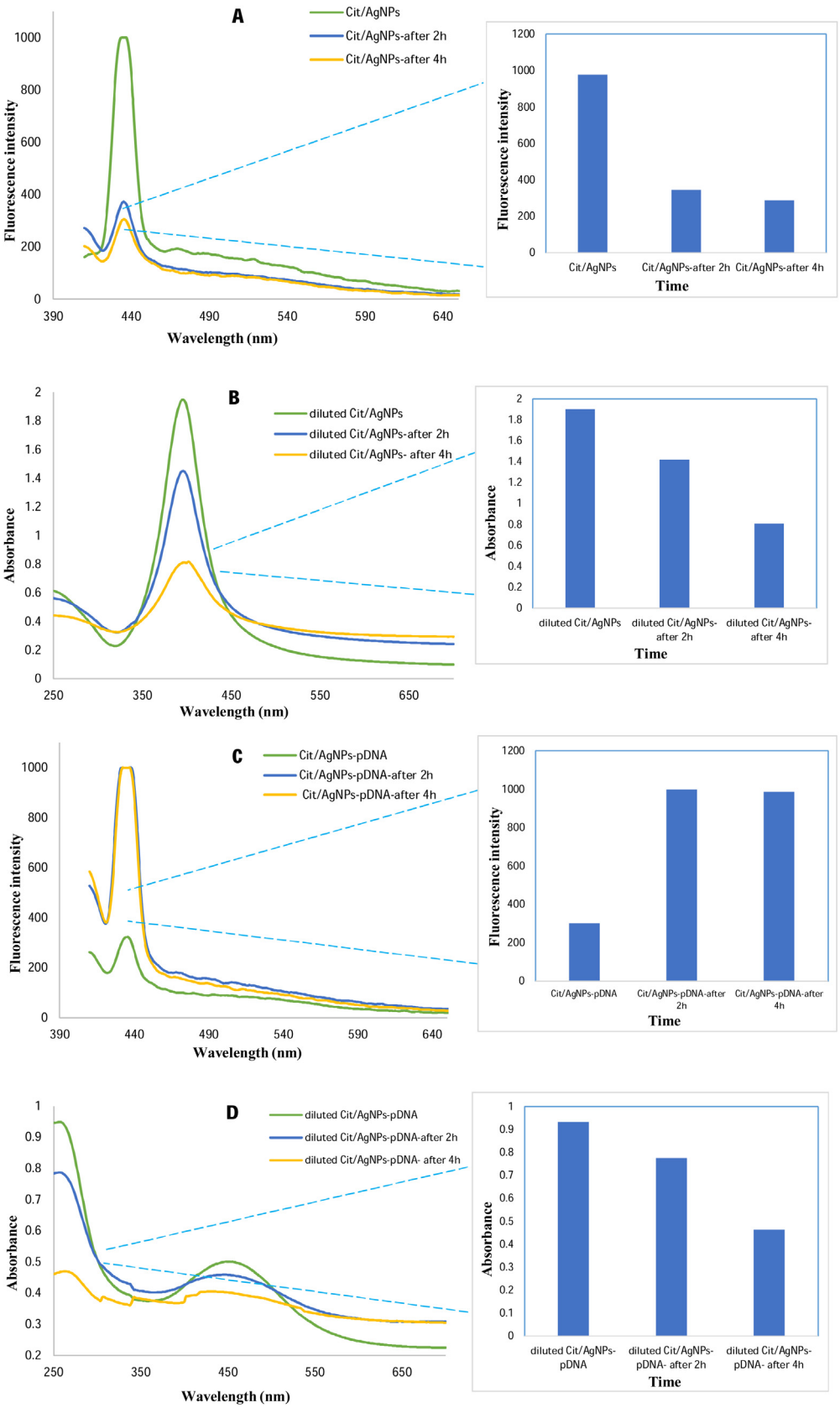

Fig. 8. Fluorescence excitation (A–C) and UV/Vis absorbance (B–D) of Cit/AgNPs and Cit/AgNPs-pDNA, respectively, at regular 2 -h interval time.

4. Conclusion

A unique method for the analysis of DNA hybridization was developed to detect *Haemophilus influenza*. The technique was based on spectrofluorometeric and UV/Vis spectrophotometric which detected hybridization of DNA using citrate capped silver nanoparticles conjugation as a transducer. The LLOQ (low limit of quantification) of DNA sample was 1 zM using 15 μL of probe and 200 μL of Cit/AgNPs. The fabricated platform not only is rapid and simple, but also it is cost-efficient, convenient and only a small volume of sample is required. Therefore, this technique has potential applications in clinical diagnosis field. Fast and specific determination of pathogenic bacteria could be a great alternative for hard-growing bacteria diagnosis.

Declaration of Competing Interest

There is no conflict of interest.

Acknowledgements

This research work was supported by Tabriz University of Medical Sciences, Tabriz, Iran.

References

[1] J.R. Gilsdorf, C.F. Marrs, B. Foxman, Haemophilus influenzae: genetic variability and natural selection to identify virulence factors, Infect. Immun. 72 (5) (2004) 2457–2461.
[2] M.P. Slack, H.J. Azzopardi, R.M. Hargreaves, M.E. Ramsay, Enhanced surveillance of invasive Haemophilus influenzae disease in England, 1990 to 1996: impact of conjugate vaccines, Pediatr. Infect. Dis. J. 17 (9) (1998) S204–S207.
[3] P.D. Butler, E.R. Moxon, A physical map of the genome of Haemophilus influenzae type b, Microbiology 136 (12) (1990) 2333–2342.
[4] J. Puri, V. Talwar, M. Juneja, K. Agarwal, H. Gupta, Prevalence of anti-microbial resistance among respiratory isolates of Haemophilus influenzae, Indian Pediatr. 36 (1999) 1029–1031.
[5] W. Kennedy, S. Chang, K. Purdy, T. Le, P. Kilgore, J. Kim, D. Anh, P. Huong, B. Dong, D. Tan, Incidence of bacterial meningitis in Asia using enhanced CSF testing: polymerase chain reaction, latex agglutination and culture, Epidemiol. Infect. 135 (7) (2007) 1217–1226.
[6] A. Mobed, M. Hasanzadeh, N. Shadjou, S. Hassanpour, A. Saadati, M. Agazadeh, Immobilization of ssDNA on the surface of silver nanoparticles-graphene quantum dots modified by gold nanoparticles towards biosensing of microorganism, Microchem. J. 152 (2020) 104286.
[7] M.L. Yola, T. Eren, N. Atar, A novel and sensitive electrochemical DNA biosensor based on Fe@ Au nanoparticles decorated graphene oxide, Electrochim. Acta 125 (2014) 38–47.
[8] M.H. Abdalhai, An.M. Fernandes, X. Xia, A. Musa, J. Ji, X. Sun, Electrochemical genosensor to detect pathogenic bacteria (Escherichia coli O157: H7) as applied in real food samples (fresh beef) to improve food safety and quality control, J. Agric. Food Chem. 63 (20) (2015) 5017–5025.
[9] S. Dash, A. Kumar, Detection of pathogenic bacteria: a genosensor approach, J Bacteriol Mycol Open Access 4 (3) (2017) 00095.
[10] R. Das, M.K. Sharma, V.K. Rao, B. Bhattacharya, I. Garg, V. Venkatesh, S. Upadhyay, An electrochemical genosensor for Salmonella typhi on gold nanoparticles-mercaptosilane modified screen printed electrode, J. Biotechnol. 188 (2014) 9–16.
[11] W. Sun, P. Qin, H. Gao, G. Li, K. Jiao, Electrochemical DNA biosensor based on chitosan/nano-V2O5/MWCNTs composite film modified carbon ionic liquid electrode and its application to the LAMP product of Yersinia enterocolitica gene sequence, Biosens. Bioelectron. 25 (6) (2010) 1264–1270.
[12] K. Wang, Y. Lei, G.-X. Zhong, Y.-J. Zheng, Z.-L. Sun, H.-P. Peng, W. Chen, A.-L. Liu, Y.-Z. Chen, X.-H. Lin, Dual-probe electrochemical DNA biosensor based on the "Y" junction structure and restriction endonuclease assisted cyclic enzymatic amplification for detection of double-strand DNA of PML/RARα related fusion gene, Biosens. Bioelectron. 71 (2015) 463–469.
[13] F. Tang, C. Wang, X. Wang, L. Li, Facile synthesis of biocompatible fluorescent nanoparticles for cellular imaging and targeted detection of Cancer cells, ACS appl, Mater. Interfaces 45 (2015) 25077–25083.
[14] C. Wang, F. Tang, X. Wang, L. Li, Self-assembly of fluorescent hybrid core–Shell nanoparticles and their application, ACS appl, Mater. Interfaces 24 (2015) 13653–13658.
[15] N.G. Bastús, F. Merkoçi, J. Piella, V. Puntes, Synthesis of highly monodisperse citrate-stabilized silver nanoparticles of up to 200 nm: kinetic control and catalytic properties, Chem. Mater. 26 (2014) 2836–2846.
[16] J. Liu, J.W.Y. Lam, B.Z. Tang, Acetylenic polymers: syntheses, structures, and functions, Chem. Rev. 109 (2009) 5799–5867.
[17] Q. Wan, Q. Huang, M. Liu, D. Xu, H. Huang, X. Zhang, Y. Wei, Aggregation-induced emission active luminescent polymeric nanoparticles: non-covalent fabrication methodologies and biomedical applications, Appl. Mater. Today 9 (2017) 145–160.
[18] L. Mao, Y. Liu, S. Yang, Y. Li, X. Zhang, Y. Wei, Recent advances and progress of fluorescent bio-/chemosensors based on aggregation-induced emission molecules, Dye. Pigment. 162 (2019) 611–623.
[19] R. Jiang, M. Liu, T. Chen, H. Huang, J. Tian, Y. Wen, Q. Cao, X. Zhang, Y. Wei. Facile construction and biological imaging of cross-linked fluorescent organic nanoparticles with aggregation-induced emission feature through a catalyst-free azide-alkyne click reaction, Dye. Pigment. 148 (2018) 52–60.
[20] H. Huang, M. Liu, Q. Wan, R. Jiang, D. Xu, Q. Huang, Y. Wen, F. Deng, X. Zhang, Y. Wei, Facile fabrication of luminescent hyaluronic acid with aggregation-induced emission through formation of dynamic bonds and their theranostic applications, Mater Sci Eng C 91 (2018) 201–207.
[21] X. Zhang, K. Wang, M. Liu, X. Zhang, L. Tao, Y. Chen, Y. Wei, Polymeric AIE-based nanoprobes for biomedical applications: recent advances and perspectives, Nanoscale 7 (2015) 11486–11508.
[22] X. Zhang, M. Liu, X. Zhang, L. Tao, Y. Chen, Y. Wei, Polymerizable aggregation-induced emission dye-based fluorescent nanoparticles for cell imaging applications, Polym. Chem. 5 (2014) 356–360.
[23] X. Zhang, X. Zhang, L. Tao, Y. Chen, Y. Wei, Fabrication of aggregation induced emission dye-based fluorescent organic nanoparticles via emulsion polymerization and their cell imaging applications, Polymer. Chem. 5 (2014) 399–404.
[24] Z. Long, M. Liu, R. Jiang, Q. Wan, L. Mao, Y. Wan, F. Deng, X. Zhang, Y. Wei. Preparation of water soluble and biocompatible AIE-active fluorescent organic nanoparticles via multicomponent reaction and their biological imaging capability, Chem. Eng. J. 308 (2017) 527–534.
[25] R. Jiang, M. Liu, C. Li, Q. Huang, H. Huang, Q. Wan, Y. Wen, Q.-Y. Cao, X. Zhang, Y. Wei, Facile fabrication of luminescent polymeric nanoparticles containing dynamic linkages via a one-pot multicomponent reaction: synthesis, aggregation-induced emission and biological imaging, Mater. Sci. Eng. C 80 (2017) 708–714.
[26] G.H. Woehrle, J.E. Hutchison, S. Özkar, R.G. FINKE, Analysis of nanoparticle transmission electron microscopy data using a public-domain image-processing program, image, Turk. J. Chem. 30 (1) (2006) 1–13.
[27] S. Wang, H. Xin, Fractal and dendritic growth of metallic Ag aggregated from different kinds of γ-irradiated solutions, J. Phys. Chem. B 104 (24) (2000) 5681–5685.
[28] H. Fissan, S. Ristig, H. Kaminski, C. Asbach, M. Epple, Comparison of different characterization methods for nanoparticle dispersions before and after aerosolization, Anal. Methods 6 (18) (2014) 7324–7334.
[29] W.W. Cleland, Dithiothreitol, a new protective reagent for SH groups, Biochemistry 3 (4) (1964) 480–482.
[30] M.C. Alliegro, Effects of Dithiothreitol on protein activity unrelated to thiol–disulfide exchange: for consideration in the analysis of protein function with Cleland's reagent, Anal. Biochem. 282 (1) (2000) 102–106.